

Surface plasmon scattering by shallow and deep surface defects

Giovanni Brucoli and L. Martín-Moreno

*Instituto de Ciencia de Materiales de Aragón and Departamento de Física de la Materia Condensada, CSIC-Universidad de Zaragoza, E-50009, Zaragoza, Spain **

Surface plasmon scattering by 1D indentations and protrusions is examined, mainly in the optical regime. The width of the defects is fixed, while its height is varied. Both individual and arrays of defects are considered. Protrusions mainly reflect the incident plasmons in the optical range. Indentations mainly radiate the incident plasmon out of plane. An indentation produces maximum reflections and out-of-plane radiation at the same wavelength, when its interaction with the incident surface plasmon is resonant. Protrusions, in general, exhibit maximum reflection and radiation at different wavelengths. Shallow arrays of either defects produce a photonic band-gap, whose spectral width can be broadened by increasing the defects height or depth. At wavelengths inside the band-gap ridge arrays reflect SPPs better than groove arrays, while groove arrays radiate SPPs better than ridge arrays.

PACS numbers:

I. INTRODUCTION

Surface Plasmon Polaritons (SPPs) are bound modes that confine light at the interface separating a metal from a dielectric. The study of surface plasmons is an active research field sometimes referred to as plasmonics^{1,2}. One of the aims of plasmonics is to control the propagation of surface plasmons by means of optical elements that could couple or decouple light to surface plasmons³⁻⁷, with the prospect of developing a new technology consisting of photonic nano-devices⁸⁻¹⁰. For this, the scattering properties of SPPs by typical configurations of scatterers should be known.

In this article, we present a comparative systematic study of scattering of surface plasmon polaritons by defects of different shapes. The defects can be either indentations of the metal surface (grooves) or protrusions on it (ridges). Some properties of ridges and grooves have been investigated in several works.¹¹⁻¹⁶ Nonetheless, a clear general picture of what configurations are best for different optical functionalities, has not yet emerged. This is because plasmonic systems, such as ridges and grooves, involve a large number of physical quantities at different scales. As a consequence, dramatic changes may result from slight variations of any of the many parameters involved: wavelength, sizes, shapes, materials, the period in arrays of defects, types of illumination and so forth.

We have previously presented a comparative study of the scattering of *shallow* ridges and grooves¹⁷, a case for which analytical expressions can be obtained. In this paper we extend that study to consider the height dependence of the scatterers, and focus on analyzing systematic changes on the scattering properties, rather than on the optimization of physical properties. We analyze the scattering of a SPP by both individual defects and arrays of defects, in order to elucidate how band-gaps effects affect the properties of individual defects. In order to reveal more clearly the differences between scattering properties of ridges and grooves, in this work we consider the simplest case of bi-dimensional defects, which

are deemed infinite in one of the dimensions parallel to the interface.

II. SCATTERING SYSTEMS

Figure 1 represents a ridge and a groove and the direction of the x and z axes. These systems are deemed infinite in the direction perpendicular to the page. The metal slab is considered to be optically thick, so the defect is effectively placed on an air-metal interface. In all calculations throughout this paper, the width (w) of all defects is fixed to the value of $w = 100nm$ (which is experimentally viable). First, we shall consider individual defects of several heights: from shallow defects to deep defects. Secondly, we shall consider arrays of ridges and grooves consisting of identical defects periodically distributed. The considered material is silver and its dielectric constant is taken from Ref.[18]. Absorption is taken into account because the size of the defects may be comparable with the SPP absorption length. The solutions are attained through the Green tensor approach, which is a standard theoretical method to solve electromagnetic scattering problems¹⁹⁻²⁶.

Both ridges and grooves will be illuminated by a surface plasmon at normal incidence, propagating in the x-direction with in-plane wavevector^{27,28} $k_p = (2\pi/\lambda) \sqrt{\varepsilon(\varepsilon + 1)^{-1}}$, where λ is the free-space wavelength.

The scattering problem is defined in terms of the fraction of the SPP energy flux carried by Transmission (T), Reflection (R) and out-of-plane Radiation (S). For economy of language, throughout the paper we shall refer to the out-of plane radiation of the impinging SPP energy flux simply as radiation. Unless otherwise stated, transmission, radiation and reflection shall be represented as a function of wavelength from a short-wavelength edge of visible light at $\lambda_1 = 500nm$ to a long-wavelength edge of near-infrared light $\lambda_2 = 1000nm$. The SPP has a penetration in the air semi-space determined by

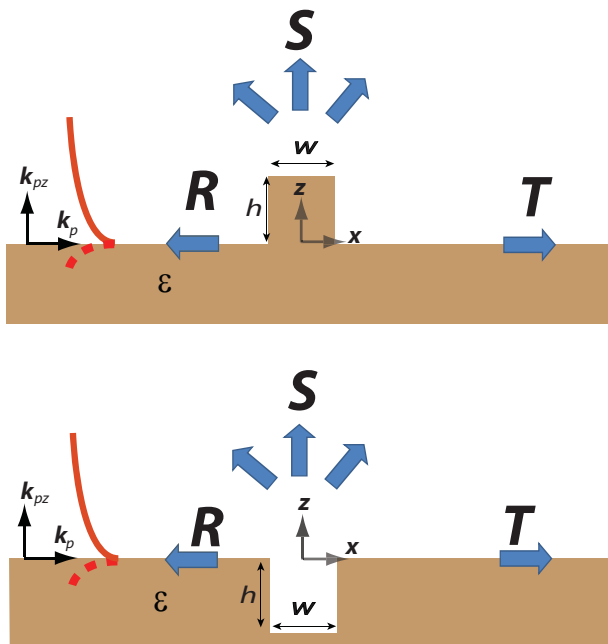


FIG. 1: Schematic representation of the two scattering systems: (a) ridges (protrusions) and (b) grooves (indentations). A surface plasmon polariton impinges at normal incidence. Part of the incident energy flux of surface plasmon is transmitted, while another part is scattered in the reflection and out-of-plane radiation channels. In this paper the width of the defects is set to $w = 100nm$.

$l_{air} = (\Im\{k_{pz}\})^{-1}$, where $k_{pz} = 2\pi/(\lambda\sqrt{\epsilon + 1})$ is the vertical component of its wavevector. In the air-silver interface, the SPP penetration in air grows monotonically from visible to infrared wavelengths, from the value of $l_{air} \simeq 200nm$ at λ_1 , to the value of $l_{air} \simeq 1080nm$ at λ_2 . Approximately at $700nm$, in the border between optical and infrared wavelengths: $l_{air} \simeq 480nm$

III. INDIVIDUAL DEFECTS

A. Individual Ridges

Figure 2 renders the evolution of the SPP transmission spectrum along with the SPP reflection and radiation spectra, of an individual ridge as its height is varied from $25nm$ to $500nm$.

The scattering by shallow defects ($h \ll \lambda$) has been previously analyzed in Ref.[17]. In this case the size of the defect is much smaller than the free-space wavelength of the incident light and, therefore, the defect scattering can be associated to the emission of a point-dipole. In 2D systems, such as shallow ridges ($h = 25nm$), R and S exhibit a smooth Rayleigh-type decay with wavelength, that scales as λ^{-3} . Correspondingly, the transmittance for shallow defects increases monotonously with wavelength. As shown in Fig. 2(a) this monotonous decrease is maintained in the case of a taller defect. The transmit-

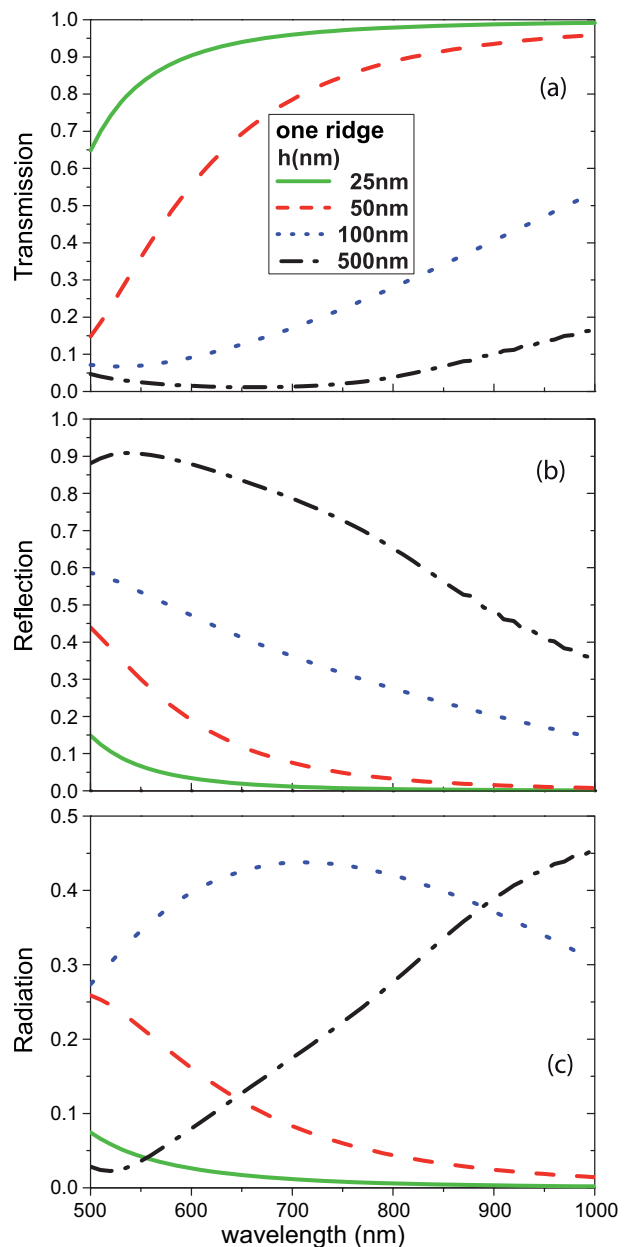


FIG. 2: (Color online) The transmission (panel (a)), reflection (panel (b)) and radiation (panel (c)) of a surface plasmon, as a function of wavelength, produced by *one ridge* at different heights. The ridge width is fixed to $w = 100nm$ while its height h is varied from $25nm$ to $500nm$. The material is silver.

tance also decrease monotonously with increasing height of the ridge, being very small ($T \sim 0.1$) when the defect height is $h \sim l_{air}/2$. As shown in Fig.2(b), the increase in h results in a monotone increase in reflection until the ridge is almost a perfect reflector, reaching its maximum efficiency of 90% of the incident plasmon (including absorption) at optical wavelengths.

Figure 2(c) shows the evolution of the radiation spectrum for the same set of heights. When the ridge is still shallow

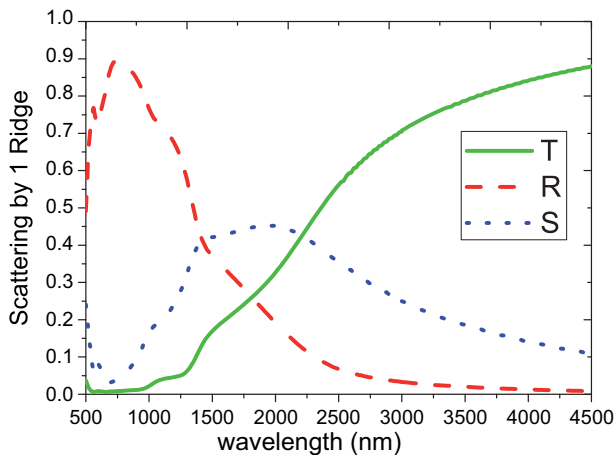


FIG. 3: (Color online) The transmission (T), reflection(R), and radiation(S) of a surface plasmon by one ridge as a function of wavelength. The ridge width is $w = 100nm$ while its height is $h = 1500nm$. The material is silver.

($h = \lambda_1/10$), the maximum radiation occurs at the lowest wavelength considered. This maximum is red-shifted at every height increment considered. Finally when the ridge height is $h = 500nm$ and $h > l_{air}$ in the optical range (up to $700nm$), the radiation peak is red-shifted to near-infrared wavelengths $\lambda > \lambda_2$. For all values of h considered, the peaks in the radiation spectrum are smaller than the maxima in the reflection spectrum.

Figure 3 represents an extremely tall ridge ($h = 1.5\mu m$). This case is perhaps difficult to reach experimentally, but it is considered for academic reasons as it contains information on the main scattering channels in different regions of the spectrum. Notice that, this time we are representing the spectra of T, R and S from a wavelength of $500nm$ to $4500nm$. In this case, reflection is the the strongest scattering channel in the optical region. Radiation, however, is the main scattering mechanism in the interval $[1500 - 2000nm]$ of the spectrum. Even then, and unlike the situation in the reflection channel, radiation is not systematically enhanced with the ridge height. In fact, its scattering efficiency never overcomes 50% of the incident energy flux.

B. Individual Grooves

The surface plasmon scattering by a groove has been studied much more than the one by a ridge, see for example Ref.[13,15,29-31]. In a simple model^{12,32} the field excited in the groove by the incident SPP can be expressed as a superposition of the waveguide modes, which propagate in the *vertical direction*. Therefore, resonances may arise due to reflection at the bottom of the groove. Thus, the scattering cross section depends strongly with h , presenting both maxima and minima (when the groove may be seen as a weak impedance defect²⁶, virtually invisible to the incident SPP). This is illustrated in Fig.4. Let us

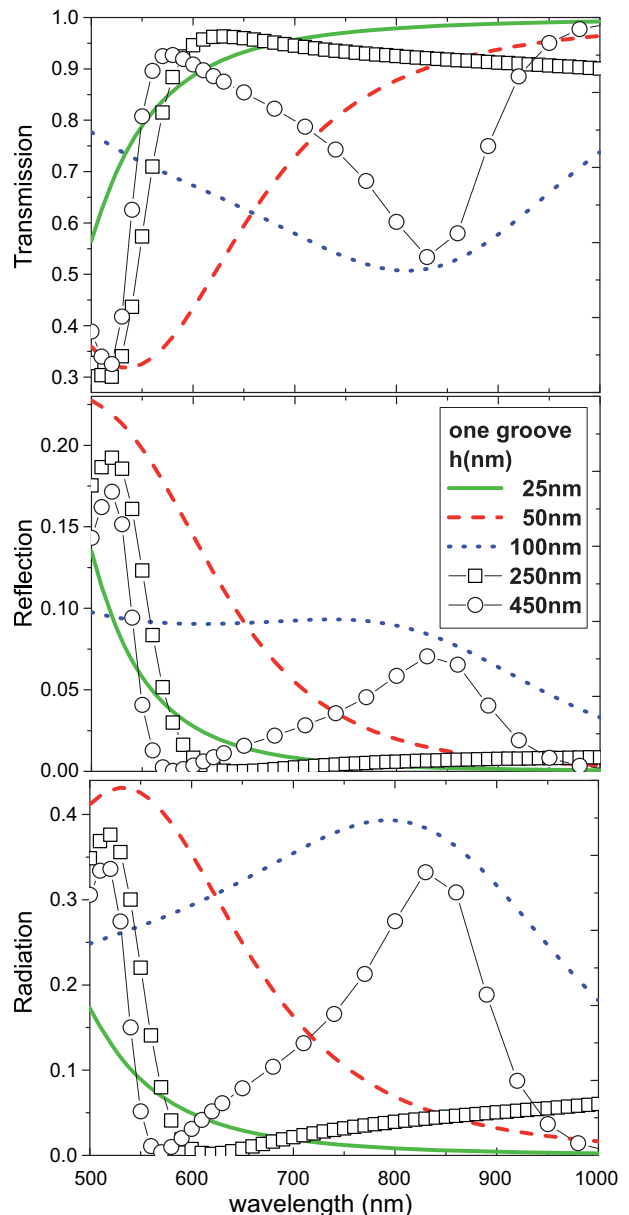


FIG. 4: (Color online) Scattering coefficients of a surface plasmon impinging onto a single groove: transmission (panel (a)), reflection (panel (b)) and radiation (panel (c)). The groove width is fixed to $w = 100nm$, but different groove depths have been considered, from $h = 25nm$ to $h = 450nm$. The material is silver.

first consider the case of a shallow groove ($h = 25nm$), which we have analyzed before¹⁷. In this case, the reflection and radiation coefficients present a Rayleigh-type monotonous decay with wavelength. However, a resonant peak appears close to $\lambda = \lambda_1 = 500nm$ already for $h = 50nm$ (i.e. $h = \lambda_1/10$). Let us label this resonance $n = 1$. Consider now $h = \lambda_1/5$. As a result of the depth increase, the groove resonance $n = 1$ is red-shifted and damped since at longer wavelengths transmission tends to increase³².

At a critical depth of a half-wavelength ($h = 250nm$) Fig.4 exhibits a new resonant wavelengths, let us label it $n = 2$. When the groove depth is further increased the $n = 2$ resonance is red-shifted (at $\simeq 850nm$) as seen for $h = 450nm$. At the same time the optical path within the groove is large enough to meet a new resonant condition ($n = 3$) in the neighborhood of λ_1 . For greater depths this behavior culminates in a multiple-resonance pattern, represented by a succession of damped and broadened oscillation between points of maximum scattering and maximum transmission as in Fig.5.

In order to show the effect of absorption on the system Fig.5 presents the spectra for T, R and S, by a $1\mu m$ deep groove with and without absorption (in this case the calculation is done by setting the imaginary part of the dielectric constant equal to zero). The figure shows that the spectral position of both the resonant wavelengths and the transmission maxima are the same in the loss-free and lossy case. Furthermore, in both cases, the net scattering (reflection+radiation) is zero at wavelengths of transmission maxima. The effect of absorption is to attenuate the amplitude of the reflection and radiation peaks at resonant wavelengths as well as those of the transmission maxima (which in the loss-free case give $T=1$).

As it turns out, the resonant coupling of the groove and the plasmon results in both radiation and reflection maxima, occurring at the same wavelengths. Yet, we find that radiation is the most efficient scattering mechanism in a groove is especially at long wavelengths, as seen for example Fig.4 and Fig.5.

The position of the transmission and scattering maxima can be calculated by making the assumption that the field propagates only in the z -direction. This assumption implies that the relation between wavelength and height at the critical points of maximum and minimum scattering (or maximum transmission) is: $h = a\lambda + b$. An estimate for a and b can be obtained by neglecting the effect of the groove width on the resonant conditions and considering that the groove is defined by walls made of perfect electrical conductor (PEC). This results in^{12,32}: $a = a_{max} = (2n + 1)/4$ and $a = a_{min} = n/2$ for for maximum and minimum scattering respectively, while $b = 0$ in both cases.

Our exact calculations are in accordance with the linear dependence between h and λ at maximum and minimum scattering, as shown in Fig.6. We have made linear fits on all resonance and transmission curves in Fig.6, calculated the relative error on them being straight lines (defined as the ratio of the standard error on the slope and the fitted slope). The relative error is always smaller than 4% in the optical range. We have tabulated the slopes and intercepts of the linear fits of our results, for the scattering maxima and minima in Table I. The exact results, is consistent with the model of Ref.[12] but shows deviations from it. This can be associated to the penetration of the field in a real metal which implies that the field inside a groove has a small wavevector component parallel to the

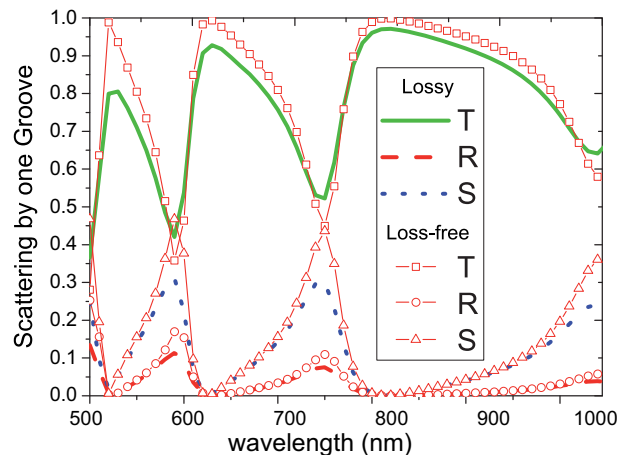


FIG. 5: (Color online) Scattering coefficients of a surface plasmon impinging onto a single groove. The groove width is $w = 100nm$ while its height is $h = 1000nm$. The material is silver (in the loss-free case the imaginary part of the dielectric constant has been set to zero).

TABLE I: The table below presents the slopes and intercepts of the linear fits of our results, for the scattering maxima and minima.

n	a_{min}	b_{min}	a_{max}	b_{max}
1	0.49	-60.8	0.188	-51.
2	0.89	-68.7	0.63	-74.
3	1.37	-128	1.05	-91.4
4	2.	-260	1.48	-113.

surface $k_x \neq 0$. Thus, while in a PEC $k_z = 2\pi/\lambda$ in a real metal k_z is larger. Correspondingly, the condition of resonant depth occurs at smaller values than those predicted by the PEC approximation. This is reflected in the smaller values obtained for the coefficients a_{min} and

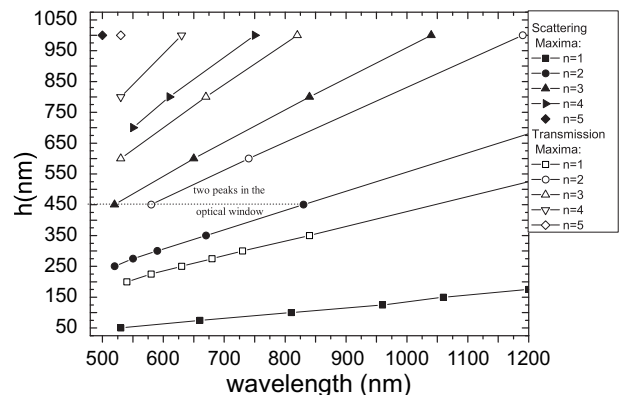


FIG. 6: The depths (h), of one groove of width $w = 100nm$, against wavelengths providing either maximum scattering or maximum transmission of SPPs. The maxima, of both transmission and scattering, that appear on the same straight line are labeled by an integer index n .

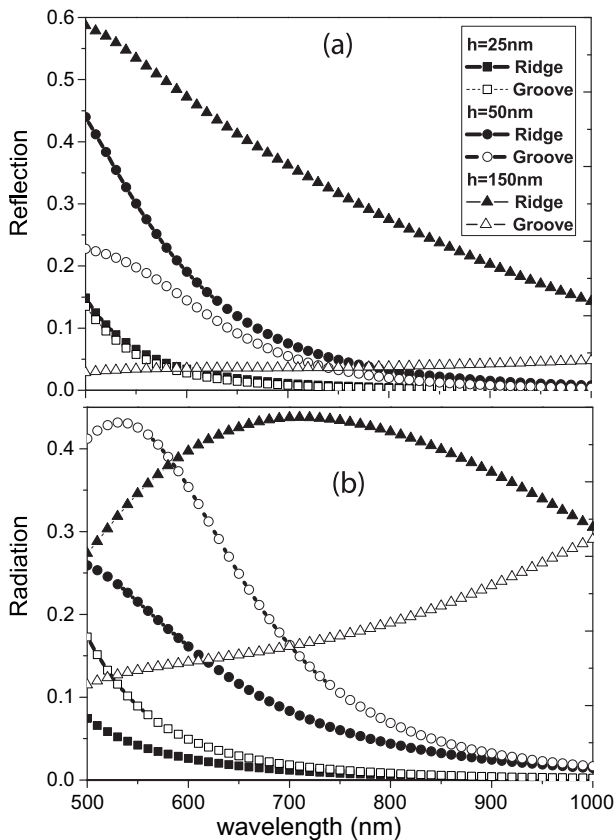


FIG. 7: The reflection (panel(a)) and radiation (panel(b)) of a surface plasmon polariton by both one ridge and one groove as a function of wavelength, for different heights/depths (h). The defects width is $w = 100nm$ while their heights are $h = 25nm, 50nm$ and $150nm$. The material is silver.

a_{max} .

IV. INDIVIDUAL RIDGES VS. INDIVIDUAL GROOVES: REFLECTION AND RADIATION

So far we have seen that the ridge capability to reflect and radiate SPPs increases systematically with height. In grooves, by contrast, reflection and radiation of SPPs occurs mainly at resonant depths.

In the Rayleigh limit the comparison between ridges and groove, revealed two limiting cases¹⁷: *i*) When the defects are very small and square, the reflection between ridges and grooves of the same size is comparable, while the out of plane radiation is always larger in a groove. *ii*) When defects are shallow but very long in the x-direction ridges and grooves have similar scattering. Yet, this requires needle-type defects, with $w \gg h$ (at least $w > 10h$). As the aspect ratio (w/h) of the defect is varied we pass gradually from the case *i*) to the case *ii*).

The scattering coefficients of the shallow defects considered ($w = 4h$), can be qualitatively associated with case *i*) as shown in Fig.7. The rest of the section is devoted

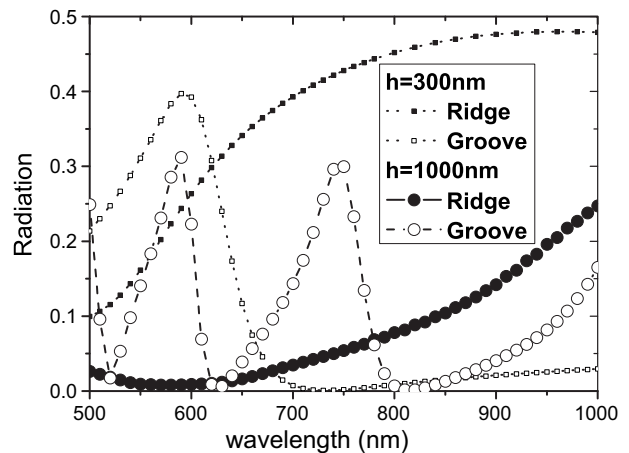


FIG. 8: The radiation of surface plasmon polaritons by both one ridge and one groove as a function of wavelength, for different heights/depths (h). The defects width is $w = 100nm$ while their heights are $h = 300nm$ and $h = 1000nm$. The material is silver.

to studying how this scenario changes when the defects are not shallow.

A. Reflection of surface plasmons

Figure 7(a) compares the reflection spectra of ridges and grooves of the same sizes, as h is increased up to $h \sim \lambda_1/3$. The figure illustrates the greater reflection efficiency of ridges over grooves, for this range of values of h . Ridges can efficiently reflect the incident SPP, even when their height is only a few tens of nanometers. Figure 7(a) shows that a $50nm$ -tall ridge, at a wavelength $\lambda = 500nm = 10h$ is able to reflect almost 45% of the incident SPP. We find that, in agreement with the results of Ref.[29], a groove never overcomes a reflection efficiency of 30% of the impinging SPP energy flux. For larger values of h than those rendered in Fig.7(a), the ridge maximum reflection efficiency is much greater than that of a groove with the same size and shape.

B. Out-of-plane Radiation of surface plasmons

The comparison between the radiation efficiency of SPPs by grooves with the one by ridges of the same size, is more complex.

Figure 7(b) shows that the groove is resonant at $\lambda = 540nm$ for $h = 50nm$. In a neighborhood of the resonant region, at optical wavelengths, the groove gives greater overall radiation than a ridge with the same size. However when the groove is non resonant ($h = 150nm$), throughout the spectral region $[\lambda_1, \lambda_2]$, its radiation is smaller than the one by the ridge, in the entire spectral region.

A second resonance of the groove emerges at $h = 300nm$.

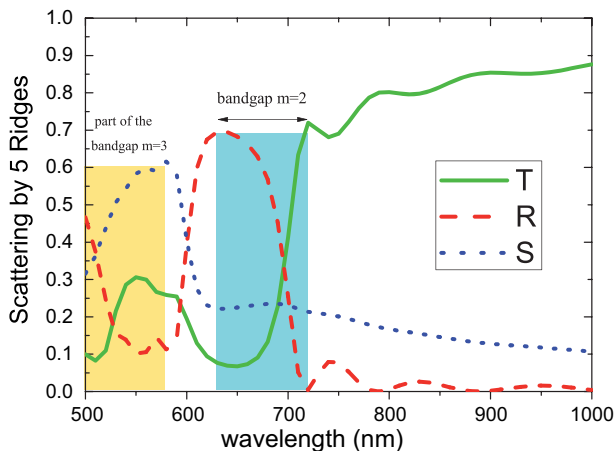


FIG. 9: (Color online) The transmission (T), reflection(R), and radiation(S) of a surface plasmon by an array of five ridges as a function of wavelength. The period is $600nm$, and each ridge has width $w = 100nm$ and height $h = 50nm$. The material is silver. The spectral positions of the band-gaps are indicated.

As seen in Fig.8 such groove resonance presents a localized peak over a relatively small spectral region in the visible range. Instead, for a ridge of the same height, the SPP radiation grows monotonously in the range $[\lambda_1, \lambda_2]$. Figure 8 also shows what happens eventually for very deep defects. The maximum of the ridge radiation spectrum red-shifts and occurs at $\lambda > \lambda_1$. The radiation spectrum of a groove tends to become prominent in the optical region, presenting a multi-resonant pattern of emission lines.

In conclusion, an individual ridge scatters the energy flux of an incident SPP, more efficiently than a groove of the same height. The related reflection and radiation spectra broaden as the ridge gets taller (but still in the range $h \ll l_{air}/2$). Radiation maxima occur at different wavelengths from reflection maxima. However a single groove presents resonances that depend on the groove depth. Resonant radiation and reflection peaks occur at the same wavelength. A resonant groove presents a larger radiation coefficient than a ridge of the same size.

V. ARRAYS OF SURFACE DEFECTS

We shall now highlight the effects exhibited collectively by arrays of either ridges or grooves, which do not appear in individual defects, and then comment briefly on the cases in which scattering is explainable in terms of the individual behavior of defects.

As known, a set of scatterers periodically distributed, exhibits photonic band-gaps^{33,34}. We have considered arrays of five *identical defects* of width $w = 100nm$, with a periodicity of $600nm$, and with height h , which is varied. As it turns out, this is a sufficient number of defects to observe band-gaps effects. The periodicity is chosen to

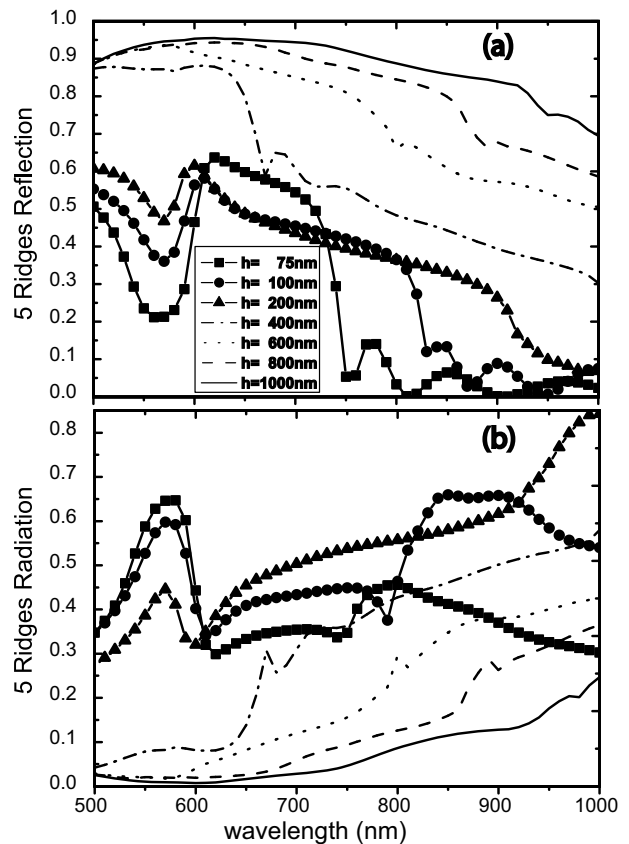


FIG. 10: (Color online) The reflection (Panel(a)) and radiation (Panel(b)) of a surface plasmon polariton by an array of five ridges (period $600nm$) as a function of wavelength, for different heights (h). Each ridge has width $w = 100nm$ while its height is varied from $h = 75nm$ to $h = 1000nm$. The material is silver.

produce band-gap effects within the optical range. Most of the phenomenological analysis, for our scattering system, is based on the concept of band-gap structure. The position of the band-gap short-wavelength edge $\lambda_-^{(m)}$ is determined by the Bragg law^{5,15,34} $k_p d = m\pi$. The width of the band-gap spans from $\lambda_-^{(m)}$ to $\lambda_+^{(m)}$. Former results^{15,16} have shown that reflection has a peak at $\lambda_-^{(m)}$ while radiation has a peak at $\lambda_+^{(m)}$.

The short-wavelength edge of the band-gap $m = 2$ is at about $\lambda_-^{(2)} \approx 630nm$. This is the main band-gap observable in our system within the spectral range $[\lambda_1, \lambda_2]$. Yet the $m = 3$ bands-gap will be part of the discussion.

A. Ridges arrays: Collective effects

For the chosen period, ridge arrays produce band-gaps that span a region within $[\lambda_1, \lambda_2]$. In Fig.9 we can notice the whole $m = 2$ band-gap $[\lambda_-^{(2)}, \lambda_+^{(2)}]$ as well as the long-wavelength edge $\lambda_+^{(3)}$ of the $m = 3$ band-gap at $550nm$.

At wavelengths in the neighborhood of $\lambda_+^{(3)}$ the impinging SPP energy is scattered mainly in the radiation channel, while in a neighborhood of $\lambda_-^{(2)}$, it goes mainly into the reflection channel. These two band-gaps are very close together. When the incident SPP free-space wavelength is just outside the $m = 3$ band-gap $\lambda > \lambda_+^{(3)}$, the main scattering mechanism becomes the build-up to the reflection maximum, up to the wavelength $\lambda_-^{(2)}$. Notice that the $m = 3$ band-gap is opened by fulfilment of Bragg's condition at about $430nm$. Yet we have not considered this region because the SPP propagation in silver, at these wavelengths, is curtailed by large absorption effects.

An increase in the height (h) of the ridges in the array results in band-gap broadening (see Fig.9). As the band-gap $m = 2$ gets larger, the reflection peak at $\lambda_-^{(2)}$ becomes more asymmetric. In fact, for a fixed h , the asymmetry in the reflection peak $\lambda_-^{(2)}$ is caused by the progressive growth of the radiation spectrum throughout the gap. The band-gap, and hence the growth of the radiation spectrum, spans from $\lambda_-^{(2)}$ to $\lambda_+^{(2)}$. If, in a different configuration, $\lambda_+^{(2)}$ is shifted to a longer wavelength $\lambda_+^{(2)'}$, the related radiation growth is also extended to $\lambda_+^{(2)'} > \lambda_+^{(2)}$, resulting in a more asymmetric reflection peak at $\lambda_-^{(2)}$. Therefore the asymmetry of the reflection peak is also associated to the spectral width of the gap. Figure 10(a) shows that if h is increased from $h = 75nm$ to $h = 200nm$, the resulting band-gap expands its width to include a broader spectral region.

Notice that the reflection spectra in Fig.10(a), exhibits a set of small multiple-resonance peaks at $\lambda > 750nm$, for $h = 75nm$ and $h = 100nm$. Correspondingly, radiation also exhibits such small peaks, in the near-infrared region of the spectra rendered in Fig.10(b). The small peaks are array finite-size effects formerly discussed in Ref.[11]. Notice that, as explained in Ref.[11], finite-size effects occur outside the band-gap edges. For $h = 400nm$ the height of the ridges is such that $h \sim l_{air}$, in the range $\lambda \in [500 - 600]nm$. At these wavelengths such arrays consist of ridges so tall that the first one or two block most of the impinging plasmon. As seen in Fig.10 when h is increased from 400 to $1000nm$, reflection rapidly becomes the only scattering channel in the range $[\lambda_1, \lambda_2]$ while radiation vanishes. Therefore, as h approaches $1000nm$, band-gap effects tend to disappear in the whole optical spectrum and the scattering of the incident SPP by the ridge array, can be interpreted, mainly, as the individual scattering of the first one or two ridges.

B. Grooves arrays: Collective effects

As found for individual grooves, the scattering coefficients of grooves arrays have an oscillatory behavior that depends on the depth of the grooves and the free-space wavelength of the incident SPP. Several works^{12,14,15,32,35,36} have studied SPP scattering by

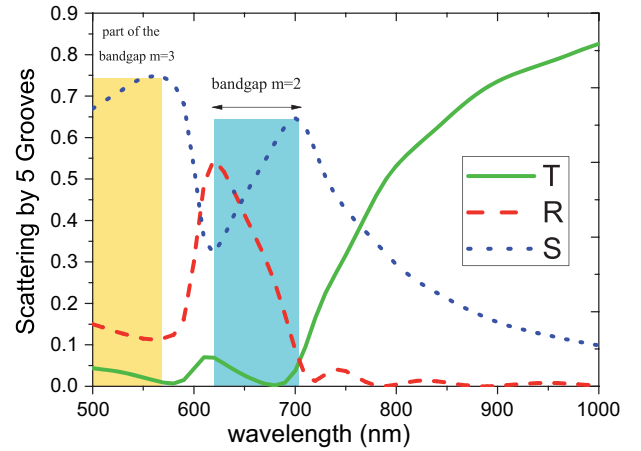


FIG. 11: (Color online) The transmission (T), reflection(R), and radiation(S) of a surface plasmon by an array of five grooves, and period $600nm$ as a function of wavelength. Each groove has a width $w = 100nm$ and depth $h = 50nm$. The material is silver. The spectral position of the band-gaps is indicated.

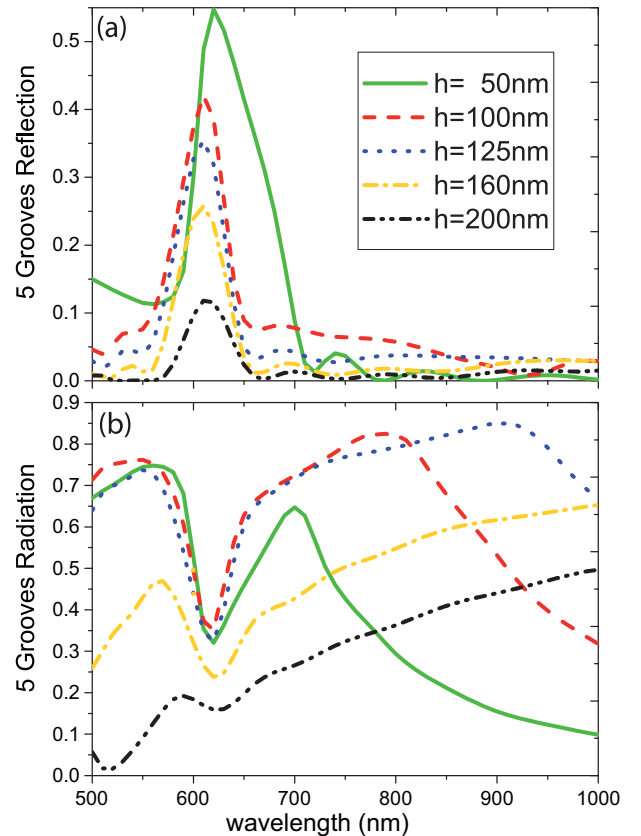


FIG. 12: (Color online) The reflection (Panel(a)) and radiation (Panel(b)) of a surface plasmon polariton by an array of five grooves, and period $600nm$, as a function of wavelength, for different depths (h). Each groove has width $w = 100nm$ while its depth is varied from $h = 50nm$ to $h = 1000nm$. The material is silver.

groove arrays. In order to compare with the ridge array analyzed before, in the following, we shall consider the SPP scattering by 5 grooves with period $600nm$ and width $100nm$, and different depths.

First of all in Fig.11 we present the exact result for the array of grooves considered in Ref.[15] with an approximate method. The two results are extremely similar, except that the radiation growth within the band-gap is much more evident in the exact result than in the approximate one. Noticeably Fig.11 features the same radiation peak at $\lambda_+(3)$ as Fig.9.

As opposed to the individual behavior of a resonant groove, in groove arrays the reflection and radiation maxima are effectively decoupled, when the grooves are interacting collectively. In fact, in this case the reflection peak is imposed at $\lambda_+^{(m)}$ by Bragg's interference, based on the period of the array. However, since the radiation peak is caused by the decrease of the reflection (and transmission) within the gap the two peaks appear at different wavelengths, unless the spectral width of the band-gap is zero.

When, in the same configuration, the depth of the grooves is increased up to $h = 200nm$, the interaction between the incident SPP and the groove weakens. As a result the related reflection maximum is systematically reduced, as seen in Fig.12(a). Figure 12(b) shows that the radiation maximum at $\lambda_+^{(3)}$ disappears. Similarly, as h increases, the radiation also vanishes throughout the spectrum $[\lambda_1, \lambda_2]$. The radiation peak at $\lambda_+^{(2)}$ is only observable for $h = 50nm$ and $h = 100nm$, while for deeper grooves it is red-shifted beyond $\lambda > \lambda_2$.

Figure 13 represents the result for very deep grooves. Note the small reflection peak at $\lambda_-^{(2)}$ is the only one decoupled from radiative emission lines. Comparison with Fig.5 suggests that the interaction between the 5 grooves in Fig.13 is weak and that the scattering produced by the array is rather a superposition of the individual behavior of each groove. The comparison between the two figures also shows that the values of radiation peaks are about 60% in Fig.13 and about 30% in Fig.5. That is, at resonance, the fraction of impinging SPP flux radiated by five grooves doubles the one radiated by a single groove, of the same size. Besides radiating more efficiently, five grooves produce more dissipation of the impinging SPP energy flux than one does, and this causes less overall transmission throughout the spectrum in Fig.13.

Finally notice that, as found for individual grooves, the out-of-plane radiative loss is the dominant scattering mechanism for groove arrays. However arrays of grooves can produce considerable reflection of surface plasmons.

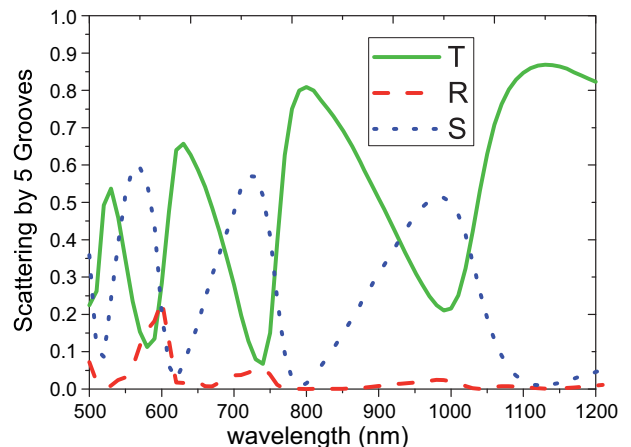


FIG. 13: (Color online) The transmission (T), reflection(R), and radiation(S) of a surface plasmon by an array of five grooves, and period $600nm$, as a function of wavelength. Each groove has a width $w = 100nm$ and depth $h = 1000nm$. The material is silver.

VI. ARRAYS OF RIDGES VS ARRAYS OF GROOVES

As seen, ridges produce larger reflection efficiencies than grooves, even when the latter are resonant.

Comparing the increase of the radiation peak at $\lambda_+^{(2)}$ in Fig.11 with that in Fig.9 suggests that grooves are better radiative emitters when the defects are shallow. Accordingly, in groove arrays the main scattering mechanism within the band-gap is radiation. In ridge arrays the main scattering mechanism within the band-gap is reflection. The spectral width of the band-gap produced by either ridges or grooves of $h = 50nm$ is practically equal. Note that grooves are not resonant within the band-gap $[\lambda_-^{(2)}, \lambda_+^{(2)}]$ for $h = 50nm$ (see Fig.6). However, for $h = 100nm$ grooves are resonant within the spectral range $[\lambda_-^{(2)}, \lambda_+^{(2)}]$. In this case the band-gap width produced by the groove array is larger than the one produced by the ridge array. In fact, in grooves $\lambda_+^{(2)} \approx 900nm$ (see Fig.12(b)), while in ridges $\lambda_+^{(2)} \approx 800nm$ (see Fig.10(a)). Deep groove arrays undergo larger dissipative loss than tall ridges, and their maximum out-of-plane scattering efficiency is about 60%. Tall ridges dissipate less of the SPP energy, achieving a maximum reflection efficiency over 90%.

VII. CONCLUSIONS

We have studied the individual and collective scattering of ridges and grooves in the optical range. The width of the defects was always fixed to a typical value of $100nm$ and the period in arrays was fixed to $600nm$, while the height and depths were varied from $25nm$ to about one micron. To the best of our knowledge this is the first

comparative treatment between ridges and grooves where their depth is systematically increased. We found ridges are very good reflectors, featuring (90%) reflection efficiency, including absorption. The related reflection becomes the main scattering channel in the optical range as the ridge height is increased, while radiation is red-shifted to infrared wavelengths. The reflection and out-of-plane radiation maxima are found at different wavelengths. Ridges produce more scattering than grooves in general, but the latter are more versatile. In fact, by adjusting their depth to the free space wavelength, we can produce a tunable resonance or virtual invisibility. At resonance grooves exhibit radiation and reflection at the same wavelength, but these can be decoupled through band-gap effects. Reflection is the least efficient mechanism for both individual and collections of grooves. In both cases the reflection peaks tend to disappear in the long-wavelength limit.

In shallow arrays ($h < 50nm$) ridges and grooves have similar band-gap structures. However, within the gap,

ridges can reflect incident SPPs more efficiently than grooves. In turn, grooves can radiate the incident SPP more efficiently than ridges. An array consisting of grooves whose depth is resonant at wavelengths within the band-gap, produces a larger band-gap spectral width than an array of ridges with the same size and period.

A SPP suffers large dissipative losses when scattered by a deep groove array, and the maximum fraction of the impinging SPP energy flux scattered by a groove array is 60%. A tall ridge array can reflect more than 90% of the impinging SPP energy flux.

VIII. ACKNOWLEDGMENTS

The authors acknowledge financial support from the Spanish Ministry of Science and Innovation under grants MAT2008-06609-C02, CSD2007-046-Nanolight.es and NO.AP2005-5185.

-
- * Electronic address: gianni@unizar.es
- ¹ S.A.Maier, *Plasmonics: Fundamental and Applications* (Springer-Verlag, New York, 2006).
 - ² A. V. Zayats, I. Smolyaninov, and A. Maradudin, *Physics Reports* **408**, 131 (2005).
 - ³ H. Ditlbacher, J. R. Krenn, N. Felidj, B. Lamprecht, G. Schider, M. Salerno, A. Leitner, and F. R. Aussenegg, *Appl. Phys. Lett.* **80**, 404 (2002).
 - ⁴ J.-C. Weeber, Y. Lacroute, A. Dereux, T. Ebbesen, C. Girard, M. González, and A. Baudrion, *Phys. Rev. B* **70**, 235406 (2004).
 - ⁵ M. U. González, J.-C. Weeber, A.-L. Baudrion, A. Dereux, A. L. Stepanov, J. R. Krenn, E. Devaux, and T. W. Ebbesen, *Phys. Rev. B* **73**, 155416 (2006).
 - ⁶ I. P. Radko, S. I. Bozhevolnyi, G. Brucoli, L. Martín-Moreno, F. J. García-Vidal, and A. Boltasseva, *Phys. Rev. B* **78**, 115115 (2008).
 - ⁷ I. P. Radko, S. I. Bozhevolnyi, G. Brucoli, L. Martín-Moreno, F. J. García-Vidal, and A. Boltasseva, *Opt. Express* **17**, 7228 (2009).
 - ⁸ E. Ozbay, *Science* **311**, 189 (2006).
 - ⁹ T. Ebbesen, C. Genet, and S. Bozhevolnyi, *Physics Today* **61(5)**, 44 (2008).
 - ¹⁰ R. Zia, J. Sculler, A. Chandran, and M. Brongersman, *Materials Today*, **9**, 20 (2006).
 - ¹¹ F. Pincemin and J.J.Greffet, *J.Opt.Soc.Am.B* **13**, No.7, 1499 (1996).
 - ¹² F.J.García-Vidal, H.J.Lezec, T.W.Ebbesen, L.Martín-Moreno, *Phys. Rev. Lett.* **90**, 213901 (2003).
 - ¹³ J.A.Sánchez-Gil and A.A Maradudin, *Opt.Express* **12(5)**, 883 (2004).
 - ¹⁴ J.A.Sánchez-Gil and A.A Maradudin, *Appl.Phys.Lett.* **86**, 251106 (2005).
 - ¹⁵ F.López-Tejeira, F.J.García-Vidal and L. Martín-Moreno, *Phys. Rev. B* **72**, 161405 (2005).
 - ¹⁶ T. Søndergaard, S. I. Bozhevolnyi, and A. Boltasseva, *Phys. Rev. B* **73**, 045320 (2006).
 - ¹⁷ G. Brucoli and L. Martín-Moreno (Resubmitted to PRB).
 - ¹⁸ E. D. Palik, *Handbook of Optical Constants of Solids* (Academic, New York, 1985).
 - ¹⁹ H.W.Hohmann, *Geophysics* **40**, 309 (1975).
 - ²⁰ G. Protásio, D. Rogers, and A. Giarola, *Radio Sci* **17**, 503 (1982).
 - ²¹ O. Keller, *Phys. Rev. B* **34**, 3883 (1986).
 - ²² L. W. Li, J. Bennet, and P. Dyson, *Int.J.Electron.* **70**, 803 (1991).
 - ²³ O. J. F. Martin, C. Girard, and A. Dereux, *Phys. Rev. Lett.* **74**, 526 (1995).
 - ²⁴ L. B. Felsen and N. Marcuvitz, *Radiation and Scattering of Waves* (IEEE Press, New York, 2003).
 - ²⁵ L.Novotny and B.Hecht, *Principles of Nano-Optics* (Cambridge University Press, Cambridge, 2006).
 - ²⁶ A. Y. Nikitin, G. Brucoli, F. J. García-Vidal, and L. Martín-Moreno, *Phys. Rev. B* **77**, 195441 (2008).
 - ²⁷ M. Cottam and D.R.Tilley, *Introduction to Surface and Superlattice Excitations* (Cambridge University Press, Cambridge, U.K., 1989).
 - ²⁸ H. Raether, *Surface Plasmons on Smooth and Rough Surfaces and on Gratings* (Springer-Verlag, Berlin, 1988).
 - ²⁹ M.Kuttge, F.J.García de Abajo and A.Polman, *Opt.Express* **17(12)**, 10385 (2009).
 - ³⁰ J.S.Q.Liu, J.S.White, S.Fan and M.L.Brongersma, *Opt.Express* **17(20)**, 17837 (2009).
 - ³¹ I. Chremmos, *J. Opt. Soc. Am. A* **27**, 85 (2010).
 - ³² F.López-Tejeira, F.J.García-Vidal and L. Martín-Moreno, *Appl.Phys.A* **89**, 251 (2007).
 - ³³ W. L. Barnes, T. W. Preist, S. C. Kitson, and J. R. Sambles, *Phys. Rev. B* **54**, 6227 (1996).
 - ³⁴ S. C. Kitson, W. L. Barnes, and J. R. Sambles, *Phys.Rev.Lett* **77**, 2670 (1996).
 - ³⁵ J. A. Sánchez-Gil, *Appl. Phys. Lett.*, **73**, 3509 (1998).
 - ³⁶ E. Hendry, F. J. Garcia-Vidal, L. Martín-Moreno, J. G. Rivas, M. Bonn, A. P. Hibbins, and M. J. Lockyear, *Phys. Rev. Lett.* **100**, 123901 (2008).